5

Watermarking Representation for Adaptive Image Classification with Radial Basis Function Network

Chi-Man Pun
University of Macau
Macau SAR
China

1. Introduction

Rapid continual advances in computer and network technologies coupled with the availability of relatively cheap high-volume data storage devices have effected the production of thousands of digital images everyday. Therefore, many content-based image retrieval (CBIR) systems have been proposed to cope with such huge image archives. To facilitate image retrieval from the huge volume image repositories, there is a great need to search for effective content-based image features. Traditionally, the most straightforward way to implement image database management systems is to make use of the conventional database-management systems (DBMS) such as relational databases or object-oriented databases. Such systems are usually keyword-based, in which the image attributes, usually in the form of text annotations, are extracted manually or partially computed and managed within the framework of a conventional DBMS, such as Chabot (Ogle and Stonebraker 1995) Piction(Srihari 1995), Photobook(Pentland, Picard et al. 1996), WebSeer(Swain, Freankel et al. 1997),etc.. However, the keyword-based approach provides limited capacity for retrieving visual information. In most cases, the associated image attributes cannot fully describe the contents of the imagery by themselves. Since the image attributes are annotated manually or semi-automatically, the process of feature extraction is extremely time-consuming and labor-intensive. Current researches on CBIR systems (Belongie, Carson et al. 1998; Gupta 1995; Smith and Chang 1996; Tao, Tang et al. 2006) mostly focus on the capability of visual search, i.e., images are retrieved based on a certain similarity criterion for a user provided sample images or sketch. These systems employ visual information indexing scheme and approximate matching instead of the exact matching used in conventional DBMS. However, most of these methods involve a high computational complexity for its feature extraction. On the other hand, with the rapid development of digital multimedia technology, different digital watermarking schemes have been proposed to address the issue of multimedia copyright protection. Many of robust watermarking schemes are using the frequency domain approach. Most of these approaches are based on discrete Fourier transform (DFT) (Pereira, Ruanaidh et al. 1999), cosine transform (DCT)

(Cox, Kilian et al. 1997; Hernandez, Amado et al. 2000; Piva, Barni et al. 1997) or wavelet transform (DWT) (Hsieh, Tseng et al. 2001 ; Pun and Kong 2007; Wang and Kuo 1998; Wang and Lin 2004), and usually have fast watermarking detection.
In this chapter, a novel approach using watermarking representation for adaptive image classification with Radial Basis Function (RBF) network is proposed. The original image is decomposed into wavelet coefficients using discrete wavelet packet transform. The energy signatures of most dominant sub-bands are extracted adaptively to form a reduced feature vector which is to be encoded as a binary watermark. The watermark is embedded by quantization into the wavelet coefficients with highest magnitudes except for those in the lowest frequency channel. Then the image features can be extracted from the watermarked image by a fast discrete wavelet packet transform and de-quantization. The extracted image features are fed to the trained RBF network for image classification. The outline of this chapter is organized as follows. In next section, we briefly introduce and review the standard 2-D discrete wavelet packets transform techniques. In section III, we present our proposed algorithm for embedding image features by watermarking and the algorithm for extracting the image features from the watermarked image. In section IV, the algorithm for adaptive image classification with RBF network is proposed. The experiment results for robustness and classification accuracy of our proposed method to various attacks, and the efficiency comparison results with other image classification method are presented in Section V. Finally, conclusions are drawn in Section VI.

2. Discrete Wavelet Packet Transform

The 2-D discrete wavelet packet transform (DWPT) is a generalization of 2D discrete wavelet transform (DWT) that offers a richer range of possibilities for image analysis. In 2D-DWT analysis, an image is split into an approximation and three detail images. The approximation image is then itself split into a second-level approximation and detail images, and the process is recursively repeated. So there are n+1 possible ways to decompose or encode the image for an n-level decomposition. In 2D-DWPT analysis, the three details images as well as the approximation image can also be split. So there are 4n different ways to encode the image, which provide a better tool for image analysis. The standard 2D-DWPT can be described by a pair of quadrature mirror filters (QMF) H and G (Mallat 1989). The filter H is a low-pass filter with a finite impulse response denoted by $h(n)$. And the high-pass G with a finite impulse response is defined by:

$$g(n) = (-1)^n h(1-n) \text{, for all n} \tag{1}$$

The low-pass filter is assumed to satisfy the following conditions for orthonormal representation:

$$\sum_n h(n)h(n+2j) = 0 \text{, for all } j \neq 0 \tag{2}$$

$$\sum_n h(n)^2 = 1 \tag{3}$$

$$\sum_n h(n)g(n+2j) = 0 \text{ , for all j} \tag{4}$$

The 2D discrete wavelet packet decomposition of an $M \times N$ discrete image x up to level p+1 ($0 \le p \le \min(\log_2(N), \log_2(M))$) is recursively defined in terms of the coefficients of level p as follows:

$$C^{p+1}_{4k,(i,j)} = \sum_m \sum_n h(m)h(n)C^p_{k,(m+2i,n+2j)} \tag{5}$$

$$C^{p+1}_{4k+1,(i,j)} = \sum_m \sum_n h(m)g(n)C^p_{k,(m+2i,n+2j)} \tag{6}$$

$$C^{p+1}_{4k+2,(i,j)} = \sum_m \sum_n g(m)h(n)C^p_{k,(m+2i,n+2j)} \tag{7}$$

$$C^{p+1}_{4k+3,(i,j)} = \sum_m \sum_n g(m)g(n)C^p_{k,(m+2i,n+2j)} \tag{8}$$

where $C^0_{0,(i,j)} = x_{(i,j)}$ is given by the intensity levels of the image x.

Since the image x has only a finite number of pixels, different methods such as symmetric, periodic or zero padding should be used for the boundary handling. At each step, we decompose the image C^p_k into four quarter-size images C^{p+1}_{4k}, C^{p+1}_{4k+1}, C^{p+1}_{4k+2} and C^{p+1}_{4k+3}.

The inverse wavelet packet transform of a discrete image x from wavelet coefficients at level p+1 can be achieved by applying recursively the following formulae until $C^0_{0,(i,j)}$ is obtained:

$$\begin{aligned} C^p_{k,(i,j)} = \; & \sum_m \sum_n h(m)h(n)C^{p+1}_{4k,(m+2i,n+2j)} + \\ & \sum_m \sum_n h(m)g(n)C^{p+1}_{4k+1,(m+2i,n+2j)} + \\ & \sum_m \sum_n g(m)h(n)C^{p+1}_{4k+2,(m+2i,n+2j)} + \\ & \sum_m \sum_n g(m)g(n)C^{p+1}_{4k+3,(m+2i,n+2j)} \end{aligned} \tag{9}$$

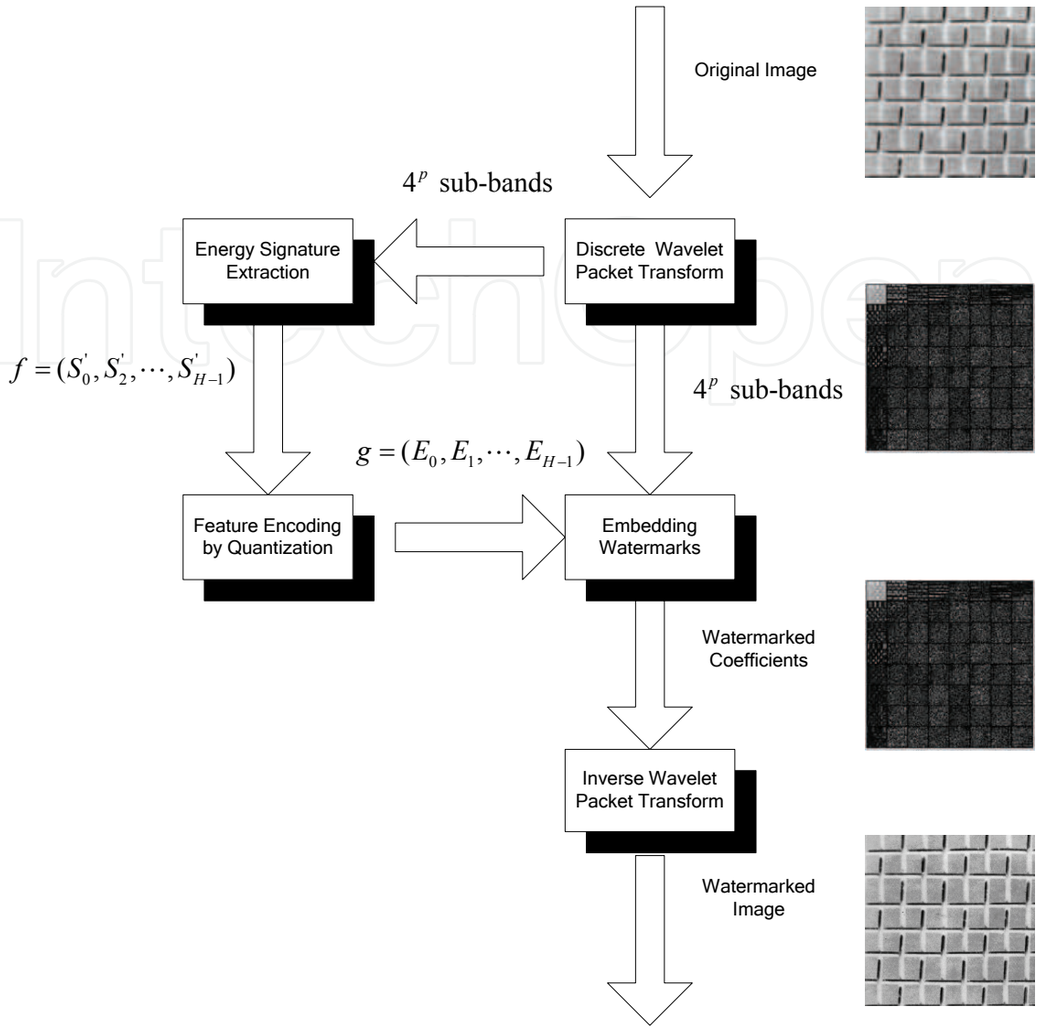

Fig.1. Procedure of embedding image features as digital watermark into the original image for image analysis.

3. Watermarking Representation of Image Features

3.1 Embedding Image Features as Digital Watermark

The procedure of embedding image features as digital watermark into the original image for image analysis or retrieval is depicted in Fig. 1. The MxN original image is decomposed into wavelet coefficients by a 2D discrete wavelet packet transform up to level p. An energy signature is computed for each sub-band of wavelet coefficients. However, the number of energy signatures for texture classification can be still very large. As suggested by Chang and Kou (Chang and Kuo 1993) the most dominant frequency sub-band provide very useful information for discriminating images. Therefore, we sort all energy signatures and choose only H most dominant energy signatures (with highest energy values) as feature vector. This feature vector is then encoded in binary feature vector, which are embedded back to the wavelet sub-bands. In order to have better perceptual invisibility, the feature vector is

embedded into the largest wavelet coefficients in each sub-band except the lowest frequency sub-band. To improve the robustness to various attacks, the same feature vector is embedded several times in remaining unused sub-bands. Finally, the inverse discrete wavelet packet transform is applied to obtain the watermarked image. The details of the algorithm are as follows:

Algorithm I: Embedding image features

Step 1. For a given $M \times N$ image, apply the p-level discrete wavelet packet transform (as described in section 2) to generate 4p sub-bands of wavelet coefficients $C^p_{k,(i,j)}$, where $p \le \log_2(N)$, $k \in \{0,\cdots,4^p-1\}$ and i, j $= 0,1,\ldots,2^{\log N - p}-1$.

Step 2. Compute an energy signature

$$S_k = \frac{1}{M \times N}\sum_{i=1}^{M}\sum_{j=1}^{N}\left|C^p_{k,(i,j)}\right|^2 \tag{10}$$

for each sub-band of wavelet coefficients $C^p_{k,(i,j)}$, where $k \in \{0,\cdots,4^p-1\}$.

Step 3. Arrange all energy signatures in descending order according to their values $S'_0, S'_1, \cdots, S'_{4^p-1}$, and choose first H most dominant energy signatures (with highest energy values) as feature vector, $f = (S'_0, S'_2, \cdots, S'_{H-1})$, where $H = \left\lfloor 4^p \big/ \alpha \right\rfloor$.

Step 4. Encode the feature vector f to a binary feature vector $g = (E_0, E_1, \cdots, E_{H-1})$ by quantization, where each energy signature S'_n is represented by En with β bits, where $n = 0,\cdots,H-1$.

Step 5. For first H sub-bands of wavelet coefficients C^p_k excluding C^p_0, embed the encoded feature En of binary feature vector $g = (E_0, E_1, \cdots, E_{H-1})$ to the largest b coefficients $C^p_{k,q}$ in the sub-band by:

$$C^p_{n,q} = \begin{cases} C^p_{n,q}, & \text{if } \left\lceil \left| \frac{C^p_{n,q}}{\Delta} \right| \right\rceil \bmod 2 = (E_n)_q \\ C^p_{n,q} = C^p_{n,q} + \Delta, & \text{if } \left\lceil \left| \frac{C^p_{n,q}}{\Delta} \right| \right\rceil \bmod 2 \neq (E_n)_q \end{cases} \tag{11}$$

where $n = 0, \cdots, H-1, q = 1, \cdots, \beta$.

Step 6. Repeat Step 5 for the next H sub-band of wavelet coefficients for $\lfloor \alpha \rfloor$ times.

Step 7. Apply the Inverse discrete wavelet packet transform (as described in section 2) to obtain the watermarked image.

3.2 Extracting the Image Features

The procedure of of extracting the image features in a watermarked image is depicted in Fig. 2. The watermarked MxN image is first decomposed into wavelet coefficients by the 2D discrete wavelet packet transform up to level p. The binary feature vector is then extracted from the sub-bands of wavelet coefficients. In order to improve the reliability, several feature vectors are extracted and combined. Finally, the image feature vector can be obtained by de-quantization for content-based image classification. The details of the algorithm are as follows:

Algorithm II: Extracting image features

Step 1. For a given $M \times N$ watermarked image, apply the p-level discrete wavelet packet transform (as described in section 2) to generate 4p sub-bands of wavelet coefficients $C^p_{k,(i,j)}$, where $p \le \log_2(N)$, $k \in \{0, \cdots, 4^p - 1\}$ and i, j = $0, 1, \ldots, 2^{\log N - p} - 1$.

Step 2. Extract the binary feature vector $g = (E_0, E_1, \cdots, E_{H-1})$ from the largest b coefficients $C^p_{n,q}$ in the sub-band n at level p by:

$$(E_n)_q = round((\sum_{i=0}^{\lfloor \alpha \rfloor - 1} \left\lceil \left| \frac{C^p_{1+n+H*i,q}}{\Delta} \right| \right\rceil \bmod 2) / \lfloor \alpha \rfloor) \qquad (12)$$

where $n = 0, \cdots, H-1, q = 1, \cdots, \beta$.

Step 3. Obtain the feature vector $f = (S'_0, S'_2, \cdots, S'_{H-1})$ from a binary feature vector $g = (E_0, E_1, \cdots, E_{H-1})$ by de-quantization, where $S'_n = E_n \times \frac{\max(S'_n)}{2^\beta}$, $n = 0, \cdots, H-1$.

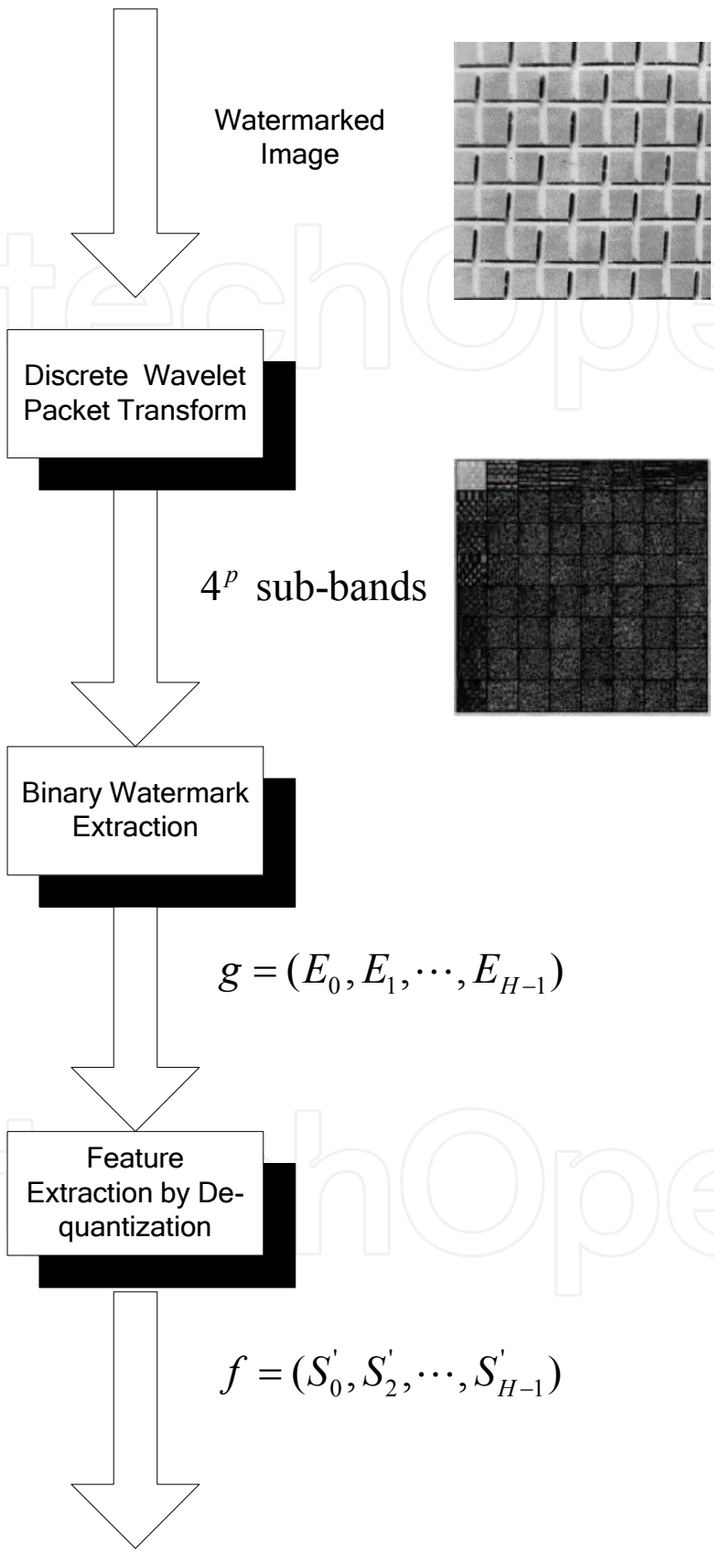

Fig.2. Procedure of extracting the image features in a watermarked image.

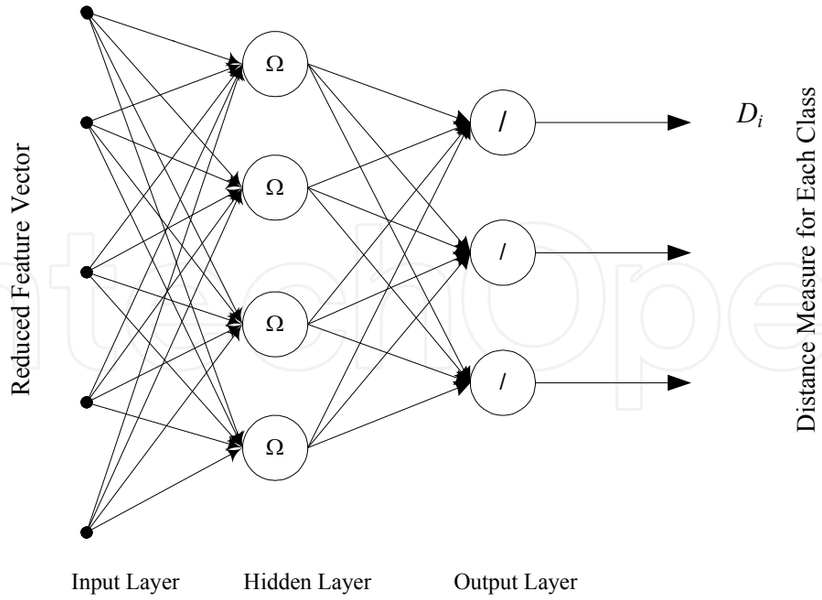

Fig. 3. Radial Basis Function (RBF) architecture.

4. Adaptive Image Classification with Radial Basis Function Network

The extracted image feature vector is used as inputs for the Radial Basis Functions (RBF) network used in the proposed adaptive classification algorithm. The RBF network involves three different layers, namely, input layer, hidden layer, and output layer, as shown in Fig. 3. The input layer is made up of a number of source / input nodes, one node for one energy signature from the reduced feature vector of a given query image. The goal of the hidden layer is to cluster the data and to further reduce its dimensionality. The output layer supplies the responses of the network to the reduced feature vector applied to the input layer during classification. The responses correspond to the distances between the input image and the different database image classes.

The proposed adaptive image classification algorithm can be divided into two stages. The first stage is for training, which is done only once. Its main objective is to construct an RBF network based on the number of features in the feature vectors and the number of classes involved, and to compute the corresponding weights of the hidden layer in the RBF network using a number of training images. The inputs to the RBF network include the feature vectors of the training image samples and their corresponding image classes. The output of the training would be the weights of the hidden layer of the network. The network starts with some initial weights which would be adjusted incrementally by the network as each feature vector and its class data are input. Therefore, the objective of the training is to produce the weights to represent the image classes of the training samples for achieving good classification results. Such weights would be used to classify query images during the classification stage. For efficiency sake, the training can be performed offline and the trained network information, including the weights, be saved for future use. The second stage is for online classification. Its main objective is to find the best match of any given query image to

one of the predefined classes captured in the trained RBF network. The details of the algorithm are as follows:

Algorithm III: Adaptive Image Classification Algorithm

Offline Training (for k training samples):

Step 1. For each training image i, compute a feature vector Ti by applying the *Algorithm II: Extracting image features*; where $i = 1, \cdots, k$.

Step 2. Construct a Radial Basis Function (RBF) network, with m input nodes, m-1 hidden nodes, and the number of output nodes being equal to the number of image classes.

Step 3. For each training image i, input the feature values of Ti and the class Cj of image i to the RBF network; use the singular value decomposition (SVD) techniques (Bishop 1995) to compute the corresponding weights of the hidden layer of the RBF network by mapping the reduced feature vector Ti to the class Cj, where $i = 1, \cdots, k$, and j =1, …, n.

Step 4. Store the trained RBF network information to secondary storage.

Online Classification:

Step 1. Load the trained RBF network information from secondary storage and reconstruct the RBF network.

Step 2. Compute a feature vector S for a query image using the *Algorithm II: Extracting image features*.

Step 3. Feed the input layer of the RBF network with the reduced feature vector S.

Step 4. Compute the outputs of the hidden unit i in the hidden layer by:

$$radbas_i = \Phi_i(\|S - \mu_i\|) = \exp\left[-\sum_{k=1}^{N} \frac{(s_k - \mu_{ik})^2}{2c_i\sigma_{ik}^2 o}\right] \tag{13}$$

where Φi is a radial basis function; ci is a proportionality constant for the variance σ_{ik}^2 ; sk is the kth component of the input vector $s = [s_1, s_2 \ldots, s_N]$, and μ_{ik} and σ_{ik}^2 are the kth components of the mean and variance vectors defining the Basis Functions (BF) respectively, and o is the overlap factor between BFs.

Step 5. Compute and output the feature distance Dj between the query texture image and class texture image j via output node j as follows:

$$D_j = \sum_i w_{ij} radbas_i + w_{0j} \tag{14}$$

where w_{ij} is the weight connecting the ith BF node to the jth output node, and w_{0j} is the threshold of the jth output node.

Step 6. Assign the query texture image to class i if $D_i \leq D_j$ for all $j \neq i$.

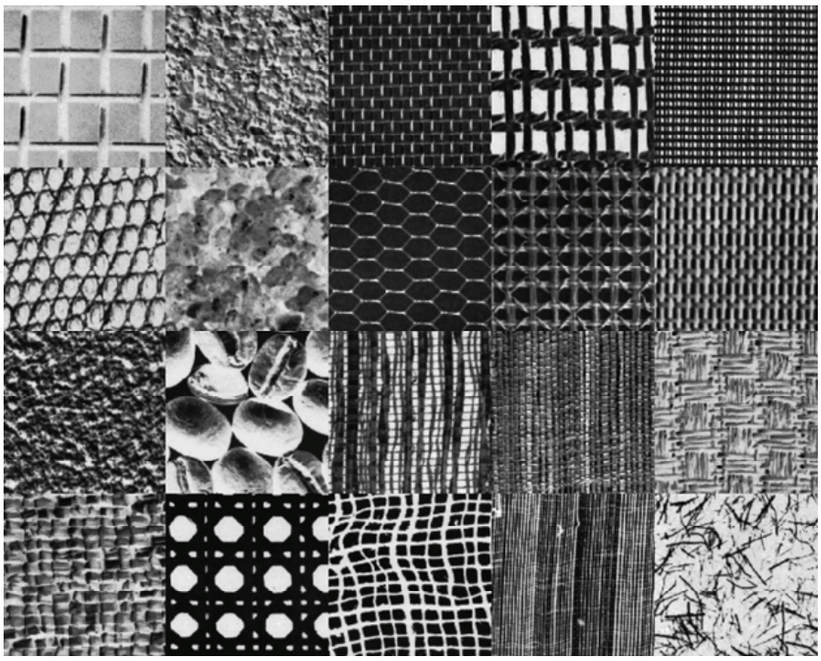

Fig. 3. Twenty class textures from Brodatz album. Row 1: D1, D4, D6, D20, D21. Row 2: D22, D28, D34, D52, D53. Row 3: D57, D74, D76, D78, D82. Row 4: D84, D102, D103, D105, D110

5. Experimental Results

In order to demonstrate the robustness and effectiveness of our proposed method, several experiments have been carried out based on a set of twenty classes of natural texture images as shown in Fig. 5, from the Brodatz's texture album (Brodatz 1996). Each texture is scanned with 150 dpi resolution, and each image, having the size 640×640 pixels and 256 gray levels, is divided into twenty-five 128×128 non-overlapping regions. So, a database of 500 (20×25) images was created for our testing. 200 of the texture images, with 10 images from each class, were used for training the RBF network, and the remaining 300 texture images form another dataset used for different watermarking and classification experiments. For embedding the image features by Algorithm I, a 20-tap Daubechies wavelet (Daubechies 1992) was used for discrete wavelet packet transform up to levels 3. The coefficients of the low-pass filter h of the 20-tap Daubechies wavelet transforms are listed in Table 1. For classification testing, a simple Euclidean classifier was used.

h(0)	0.01885858	h(10)	-0.02082962
h(1)	0.13306109	h(11)	0.02348491
h(2)	0.37278754	h(12)	0.00255022
h(3)	0.48681406	h(13)	-0.00758950

h(4)	0.19881887	h(14)	0.00098666
h(5)	-0.17666810	h(15)	0.00140884
h(6)	-0.13855494	h(16)	-0.00048497
h(7)	0.09006372	h(17)	-0.00008235
h(8)	0.06580149	h(18)	0.00006618
h(9)	-0.05048329	h(19)	-0.00000938

Table 1. 20-tap Daubechies wavelet transform filter coefficients.

First, we evaluate the perceptual quality of the watermarked images using the images in our database. Fig. 5 shows the original and the watermarked D1 image, which was embedded with 15 image features ($\alpha = 4.27$) encoded in 5 bits ($\beta = 5$). The two images are visually indistinguishable with PSNR is 41.5 dB.

Second, the experiments for verifying the robustness and classification accuracy of our method are carried out. Fig. 5 shows the watermarked D1 image attacked by Gaussian noise, JPEG compression and median filter. Table 2 shows the classification accuracy and robustness of our method for different attacks and number of dominant energy features. From the table, it was shown that the common attacks such as Gaussian noise, JPEG, and median filtering has only little effect on the classification performance. Our method has strong resistance to noise and JPEG compression with very low quality factor. The best performance was obtained using 47 features with 96.8% accuracy. The results also indicate that a higher number of dominant energy features does not imply a higher accuracy rate.

Third, the algorithm efficiency of our method was compared with other image classification method. Table 3 shows that our proposed method achieved the same classification accuracy, while having much lower complexity than other texture classification method such as wavelet packet signature method (Laine and Fan 1993).

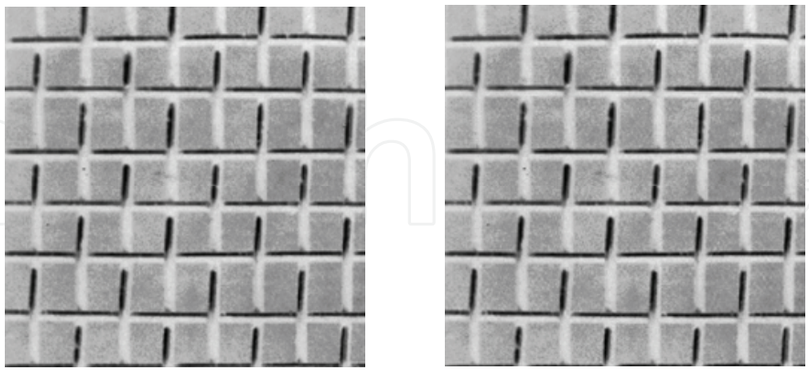

(a) (b)

Fig. 4. (a) The original D1 image; (b) Watermarked D1 image with Δ=33 , α = 4.27 , β = 5 ,PSNR=41.5 dB.

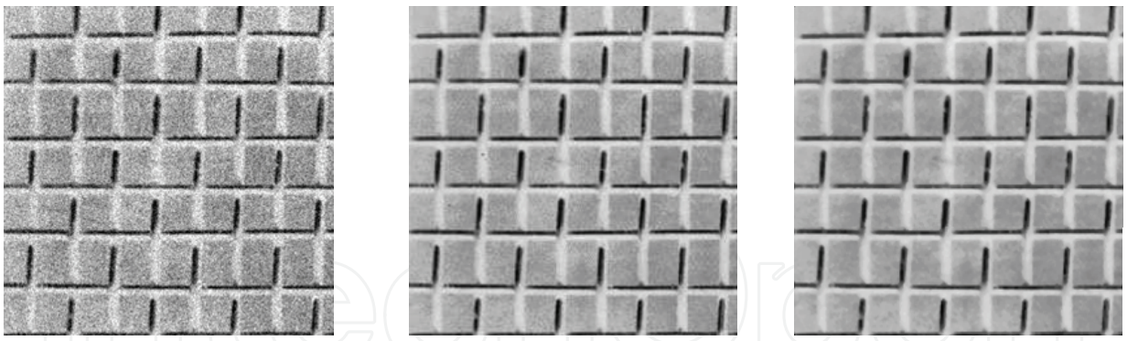

(a) (b) (c)

Fig. 5. Watermarked D1 image in Fig 4(b) attacked by (a) Gaussian noise 0.01; (b) JPEG quality factor 50; (c) 3x3 median filter.

Attacks	Number of image features					
	15	23	31	47	55	63
Gaussian Noise (0,0.01)	86.5	90.5	92.6	94.5	93.2	92.8
JPEG (QF = 50)	85.5	89.6	92.5	94.3	93.3	93.3
JPEG (QF = 30)	82.6	86.4	90.2	92.1	91.8	90.2
3x3 median filter	71.5	75.6	76.3	76.3	76.1	75.8
No attack	89.2	93.8	95.3	96.8	95.6	95.4

Table 2. Classification accuracy (%) with different attacks and number of image features.

	Proposed	WPS
Accuracy (%)	96.8	95.6
Complexity	$O(n)$	$O(n^2)$

Table 3. Performance comparison with the wavelet packet signature method.

6. Conclusion

In this chapter, a novel approach using watermarking representation for adaptive image classification with Radial Basis Function (RBF) network has been proposed. Experimental results show that the proposed method has strong resistance to noise and JPEG compression with very low quality factor, and has much better efficiency than the other image classification method. However, the performance for median filtering attacks still needs to be improved further. For image classification experiments, the best performance was obtained using only 47 features with 96.8% accuracy. Future work may focus on embedding more useful image features such as invariant features for image analysis.

Acknowledgments

This work was supported in part by the Research Committee of the University of Macau.

7. References

Belongie, S., C. Carson, et al. (1998). Color- and Texture-Based Image Segmentation using EM and Its Application to Content-Based Image Retrieval. *Proceedings of the Sixth International Conference on Computer Vision*, pp. 675

Bishop, C. (1995). *Neural Networks for Pattern Recognition* Clarendon Press. Oxford

Brodatz, P. (1996). *Texture: A Photographic Album for Artists and Designers*. Dover

Chang, T. and C. C. J. Kuo (1993). Texture analysis and classification with tree-structured wavelet transform. *IEEE Trans. Image Processing*, vol. 2, no. 4, pp. 429-441.

Cox, I. J., J. Kilian, et al. (1997). Secure spread spectrum watermarking for multimedia. *IEEE Trans. Image Processing*, vol. 6, pp. 1673-1687.

Daubechies, I. (1992). Ten Lectures on Wavelets. *CBMS-NSF Regional Conference Series in Applied Mathematics*, SIAM Press, Philadelphia, Pennsylvania.

Gupta, G. (1995). *Visual information retrieval technology - a Virage perspective.* White paper, Virage Inc

Hernandez, J. R., M. Amado, et al. (2000). DCT-domain watermarking techniques for still image: Detector performance analysis and a new structure. *IEEE Trans. Image Processing*, vol. 9, pp. 55-68.

Hsieh, M.-S., D.-C. Tseng, et al. (2001). Hiding digital watermarks using multiresolution wavelet transform. *IEEE Trans. Industrial Electronics*, vol. 48 no. 5, pp. 875 - 882.

Laine, A. and J. Fan (1993). Texture classification by wavelet packet signatures. *IEEE Trans PAMI*, vol. 15, no. 11, pp. 1186-1191.

Mallat, S. (1989). A theory for multiresolution signal decomposition: The wavelet decomposition. *IEEE Trans. PAMI*, vol. 11, no. 7, pp. 674-693.

Ogle, V. and M. Stonebraker (1995). Chabot: Retrieval from a Relational Database of Images *Computer*, vol. 28, no. 9, pp. 40-48.

Pentland, A., R. W. Picard, et al. (1996). Photobook: Content-Based Manipulation of Image Databases. *International Journal of Computer Vision*, vol. 18, no. 3, pp. 233-254.

Pereira, S., J. J. K. Ó. Ruanaidh, et al. (1999). Template based recovery of Fourier-based watermarks using log-polar and log-log maps. *IEEE Int. Conf. Multimedia Computing and Systems*, pp. 870-874.

Piva, A., M. Barni, et al. (1997). DCT-based watermark recovering without resorting to the uncorrupted original image. *IEEE Int. Conf. Image Processing*, pp. 520-527.

Pun, C.-M. and I.-K. Kong (2007). Adaptive Quantization of Wavelet Packet Coefficients for Embedding and Extraction of Digital Watermarks. *International Journal of Communications* vol. 1, no. 3, pp. 114-119.

Smith, J. and S. F. Chang (1996). VisualSEEk: a fully automated content-based image query system. *Proceeding of ACM Multimedia 96*, pp. 87-98.

Srihari, R. K. (1995). Automatic indexing and content-based retrieval of captioned images. *Computer*, vol. 28, no. 9, pp. 49-56.

Swain, M. J., C. Freankel , et al. (1997). WebSeer: An Image Search Engine for the World Wide Web. *Proceedings of the IEEE Conference on Computer Vision and Pattern Recognition* pp.

Tao, D., X. Tang, et al. (2006). Direct Kernel Biased Discriminant Analysis: A New Content-Based Image Retrieval Relevance Feedback Algorithm. *IEEE TRANS. MULTIMEDIA*, vol. 8, no. 4, pp. 716-727.

Wang, H.-J. and C.-C. J. Kuo (1998). Image protection via watermarking on perceptually significant wavelet coefficient. *IEEE 2nd Workshop Multimedia Signal Processing*, pp. 279-284.

Wang, S.-H. and Y.-P. Lin (2004). Wavelet tree quantization for copyright protection watermarking. *IEEE Trans. Image Processing*, vol. 13 pp. 154 -165.

Machine Learning

Edited by Yagang Zhang

ISBN 978-953-307-033-9
Hard cover, 438 pages
Publisher InTech
Published online 01, February, 2010
Published in print edition February, 2010

Machine learning techniques have the potential of alleviating the complexity of knowledge acquisition. This book presents today's state and development tendencies of machine learning. It is a multi-author book. Taking into account the large amount of knowledge about machine learning and practice presented in the book, it is divided into three major parts: Introduction, Machine Learning Theory and Applications. Part I focuses on the introduction to machine learning. The author also attempts to promote a new design of thinking machines and development philosophy. Considering the growing complexity and serious difficulties of information processing in machine learning, in Part II of the book, the theoretical foundations of machine learning are considered, and they mainly include self-organizing maps (SOMs), clustering, artificial neural networks, nonlinear control, fuzzy system and knowledge-based system (KBS). Part III contains selected applications of various machine learning approaches, from flight delays, network intrusion, immune system, ship design to CT and RNA target prediction. The book will be of interest to industrial engineers and scientists as well as academics who wish to pursue machine learning. The book is intended for both graduate and postgraduate students in fields such as computer science, cybernetics, system sciences, engineering, statistics, and social sciences, and as a reference for software professionals and practitioners.

InTech Europe
University Campus STeP Ri
Slavka Krautzeka 83/A
51000 Rijeka, Croatia
Phone: +385 (51) 770 447
Fax: +385 (51) 686 166
www.intechopen.com

InTech China
Unit 405, Office Block, Hotel Equatorial Shanghai
No.65, Yan An Road (West), Shanghai, 200040, China
中国上海市延安西路65号上海国际贵都大饭店办公楼405单元
Phone: +86-21-62489820
Fax: +86-21-62489821

IntechOpen